Development 133, 2747-2756 (2006) doi:10.1242/dev.02447

The *C. elegans* MELK ortholog PIG-1 regulates cell size asymmetry and daughter cell fate in asymmetric neuroblast divisions

Shaun Cordes[1], C. Andrew Frank[1,*] and Gian Garriga[1,2,†]

In the nematode *Caenorhabditis elegans*, neurons are generated from asymmetric divisions in which a mother cell divides to produce daughters that differ in fate. Here, we demonstrate that the gene *pig-1* regulates the asymmetric divisions of neuroblasts that divide to produce an apoptotic cell and either a neural precursor or a neuron. In *pig-1* mutants, these neuroblasts divide to produce daughters that are more equal in size, and their apoptotic daughters are transformed into their sisters, leading to the production of extra neurons. PIG-1 is orthologous to MELK, a conserved member of the polarity-regulating PAR-1/Kin1/SAD-1 family of serine/threonine kinases. Although MELK has been implicated in regulating the cell cycle, our data suggest that PIG-1, like other PAR-1 family members, regulates cell polarity.

KEY WORDS: Asymmetric cell division, Neuroblast, MELK, PAR-1, PIG-1, HAM-1, Cell polarity, Cell fate, Programmed cell death, Apoptosis

INTRODUCTION

Much of metazoan cellular diversity is generated by asymmetric cell divisions in which a polarized mother cell divides to produce daughters that adopt different fates (Horvitz and Herskowitz, 1992). The *C. elegans* zygote requires the serine/threonine kinase PAR-1 to establish polarity along the presumptive anteroposterior (AP) axis. Loss of PAR-1 activity disrupts asymmetric positioning of the mitotic spindle and the asymmetric distribution of cell fate determinants to daughter cells (Guo and Kemphues, 1995; Kemphues et al., 1988). PAR-1 orthologs in other organisms also regulate cell polarity. In *Drosophila*, PAR-1 polarizes the microtubule cytoskeleton in the germ line and establishes the embryonic AP axis by regulating the asymmetric localization of cell fate determinants in the oocyte (Cox et al., 2001; Shulman et al., 2000; Tomancak et al., 2000). PAR-1 also regulates epithelial polarity, both in the *Drosophila* follicular epithelium (Doerflinger et al., 2003) and in cultured MDCK cells (Cohen et al., 2004).

PAR-1 is a member of a superfamily of serine/threonine kinases that regulate cell polarity. In addition to PAR-1, this group includes Kin1p from *Schizosaccharomyces pombe* and the conserved SAD-1 family. Kin1p regulates bipolar growth and the correct positioning of the nucleus and cell cleavage plane (Drewes and Nurse, 2003; La Carbona et al., 2004). Nematode SAD-1 may regulate neural polarity (Crump et al., 2001), and the mouse homologs of SAD-1 are required for neurons to develop processes with normal dendritic and axonal properties (Kishi et al., 2005). Expression of vertebrate PAR-1 homologs in *S. pombe* can partially rescue *kin1* phenotypes, suggesting an ancestral role for this kinase family in regulating cell polarity (Drewes and Nurse, 2003).

[1]Molecular and Cell Biology, University of California, Berkeley, CA 94720, USA.
[2]Helen Wills Neuroscience Institute, University of California, Berkeley, CA 94720, USA.

*Present address: Department of Biochemistry and Biophysics, University of California, San Francisco, CA 94143-2822, USA
†Author for correspondence (e-mail: garriga@berkeley.edu)

Accepted 16 May 2006

Another member of the PAR-1/Kin1/SAD-1 superfamily of serine/threonine kinases is Maternal Embryonic Leucine zipper Kinase (MELK), also known as pEg3 kinase and MPK38 (Blot et al., 2002; Gil et al., 1997; Heyer et al., 1997). MELK proteins share sequence homology and a similar domain architecture with PAR-1 family members. Both contain an N-terminal kinase domain and a C-terminal kinase-associated region. MELK was originally identified in a screen for maternal genes expressed during pre-implantation of the mouse embryo (Heyer et al., 1997). MELK is also expressed in other vertebrate tissues, especially in proliferating cell populations, including the blast cells of the early embryo (Heyer et al., 1999), embryonic stem cells (Nakano et al., 2005), adult germ cells (ovaries and spermatogonia) (Heyer et al., 1999), hematopoietic stem cells (Easterday et al., 2003; Saito et al., 2005) and neural stem cells (Easterday et al., 2003; Nakano et al., 2005). MELK has been implicated in the regulation of spliceosome assembly (Vulsteke et al., 2004), gene expression (Saito et al., 2005) and cell proliferation (Davezac et al., 2002; Gray et al., 2005; Nakano et al., 2005). Its role in regulating cell division is controversial, with conflicting evidence suggesting it has both stimulatory and inhibitory functions.

In a screen for *C. elegans* mutants with defective asymmetric neuroblast divisions, we identified alleles of the gene *pig-1* (*par-1-like gene*), which encodes the worm ortholog of MELK. We show that PIG-1 controls cell size asymmetry and neuroblast daughter cell fate in certain neuroblast lineages. PIG-1 acts cell autonomously in affected lineages, and we propose that PIG-1 regulates asymmetric neuroblast divisions by controlling neuroblast polarity. These data are the first to implicate MELK family proteins in regulating cell polarity.

MATERIALS AND METHODS

C. elegans genetics

Nematodes were cultured as previously described (Brenner, 1974). N2 Bristol was the wild-type strain used in this study, and experiments were performed at 20°C. The following mutations and transgenic arrays were used.

LG I: *ynIs45* [*Pflp-15::gfp*] (Kim and Li, 2004), *zdIs5* [*mec-4::gfp*] (Clark and Chiu, 2003), *kyIs39* [*Psra-6::gfp*] (Troemel et al., 1995);

LG II: *ynIs25* [*Pflp-12::gfp*] (Kim and Li, 2004; Li et al., 1999a), *rrf-3(pk1426)* (Simmer et al., 2002), *juIs76* [*Punc-25:gfp*] (Jin et al., 1999), *gmIs20* [*hlh-14::gfp*] (Frank et al., 2003);
LG III: *gmIs12* [*Psrb-6::gfp*] (Hawkins et al., 2005; Troemel et al., 1995);
LG IV: *pig-1 (gm280, gm300, gm301, gm344*) (this study), *ced-3(n717)* (Ellis and Horvitz, 1986), *ham-1(n1811, n1438, gm214, gm279)* (Desai et al., 1988; Frank et al., 2005; Guenther and Garriga, 1996);
LG V: *egl-1(n1084 n3082)* (Conradt and Horvitz, 1998), *ayIs9* [*Pegl-17::gfp*] (Branda and Stern, 2000), *muIs102* [*Pgcy-32::gfp*] (Yu et al., 1997) (Y. Lie and C. Kenyon, personal communication). *gmIs22* [*nlp-1::gfp*] (Frank et al., 2003; Li et al., 1999b);
Unmapped: *mgIs21* [*Plin-11::gfp*] (Hobert et al., 1998); and
Extrachromosomal arrays: *gmEx320* and *gmEx321* [*Ppig-1::gfp; rol-6(d)*], *gmEx326* [*Ppig-1::pig-1::gfp; rol-6(d)*], *gmEx394*, *–95*, and *–96* [*Pmab-5::pig-1::gfp; Pdpy-30::NLS::dsRed2; rol-6(d)*] (this study).

Isolation of *pig-1* mutations

The *pig-1* alleles *gm280*, *gm300* and *gm301* were isolated in forward genetic screens for mutations that altered the number of PHB neurons. Mutagenesis was carried out as described by Brenner (Brenner, 1974). Mutagenized *gmIs12* P0 worms were allowed to lay eggs. After several days, we transferred 50 F1 animals onto fresh plates. From each plate we transferred 20 F2 hermaphrodites to individual plates and screened their progeny. We screened the progeny of 2400 F2 hermaphrodites.

pig-1(gm344) was isolated from a library of worms mutagenized with UV- trimethylpsoralen. The construction of this mutant library has been described (Withee et al., 2004). The *gm344* breakpoints are defined by the following two sequences that flank the 524 bp deletion: 5′-AGCTC-GTGTCAGGACGCGAA-3′ and 5′-TGGCCACCTTTTGATTTGTC-3′.

Detection and analysis of specific neurons

The HSN and NSM neurons were detected by staining adult hermaphrodites with rabbit anti-serotonin antibodies as previously described (Garriga et al., 1993). All other neurons were detected with the following integrated transcriptional reporters that express GFP under control of the indicated *C. elegans* promoter. PHB neurons: *gmIs12* [*Psrb-6::gfp*] (Hawkins et al., 2005; Troemel et al., 1995), which is expressed both in PHB and the adjacent PHA neurons, and *gmIs22* [*nlp-1::gfp*], which is PHB-specific (Frank et al., 2003; Li et al., 1999b). PHA, I2 and CAN neurons: *ynIs45* [*flp-15::gfp*] (Kim and Li, 2004). AQR, PQR and URX neurons: *muIs102* [*Pgcy-32::gfp*] (Yu et al., 1997) (Y. Lie and C. Kenyon, personal communication). ALM, AVM, PVM and PLM neurons: *zdIs5* [*mec-4::gfp*] (Clark and Chiu, 2003). SDQ, SMBD and SMBV neurons: *ynIs25* [*flp-12::gfp*] (Kim and Li, 2004; Li et al., 1999a). M4 neuron: *ayIs9* [*Pegl-17::gfp*] (Branda and Stern, 2000). PVQ neuron: *kyIs39* [*Psra-6::gfp*] (Troemel et al., 1995). VC neurons: *mgIs21* [*Plin-11::gfp*] (Hobert et al., 1998). VD and DD neurons: *juIs76* [*unc-25::gfp*] (Jin et al., 1999).

Immunostaining, dye filling and microscopy

Live animals were observed as previously described (Sulston and Horvitz, 1977). Embryos were fixed and stained as described by Guenther and Garriga (Guenther and Garriga, 1996). Dye filling of the phasmid neurons with DiI was performed as previously described (Hedgecock et al., 1987). Worms were examined using a Zeiss Axioskop 2 microscope. Images were collected using an ORCA-ER CCD camera (Hammamatsu) and Openlab imaging software (Improvision). Images were prepared for publication using Adobe PhotoShop (Adobe Systems).

Lineage analysis

L1 animals expressing *zdIs5*[*mec-4::gfp*] were mounted and followed by Nomarski optics as previously described (Sulston and Horvitz, 1977). We began following the left or right Q lineage in animals where the Q cell had divided once. After observing an animal, it was transferred to a plate with food. When the animal reached the L4 stage, we used epifluorescence to score the number of A/PVM neurons.

Cloning PIG-1

Single nucleotide polymorphism mapping was used to position *pig-1* on the left arm of LG IV between snp_Y38C1A.2 and snp_K11H12.1 (Wicks et al., 2001). We then used RNAi to systematically inactivate each of the ORFs in this region by feeding bacterial strains expressing dsRNA complementary to these ORFs to *gmIs12; ced-3(n717)* hermaphrodites (Kamath et al., 2001; Timmons and Fire, 1998). RNAi feeding strains used to inactivate genes in this region were obtained from the library designed by the Ahringer Laboratory (Fraser et al., 2000).

Analysis of *pig-1* transcripts

We characterized the transcript produced by the *pig-1* open reading frame by sequencing eight cDNA clones (yk554F7, yk338H11, yk400B12, yk150E3, yk13C10, yk88F11, yk516B10, yk167G5) kindly provided by Y. Kohara (National Institute of Genetics, Mishima, Japan). To characterize the 5′ terminus of the *pig-1* message, we amplified a *pig-1* cDNA from an oligo(dT)-primed embryonic cDNA library using the SL1 splice-leader-specific forward primer pSL1 (5′-GGTTTAATTACCCAAGTTTG-3′) and a *pig-1*-specific reverse primer W03G16N (5′-gagatccacaacacgtatcc-3′). Sequencing this PCR product revealed that SL1 is trans-spliced to the *pig-1* message one nucleotide upstream of the *pig-1* start codon.

Protein sequence analysis

Sequence alignments were performed using ClustalX (Thompson et al., 1997) and dendograms were generated with NJplot (Perriere and Gouy, 1996). The GenBank Accession numbers for sequences used in phylogenetic analyses are: *Homo sapiens* MELK, NP_055606; MARK2 (PAR-1), NP_059672; SAD1A, AAS86442; SAD1B, AAS86443; *Mus musculus* MELK, NP_034920; *Xenopus laevis* pEG3 (MELK), CAA78913; *Danio rerio* MELK, BAC75706; *C. elegans* PAR-1, NP_001024019; PIG-1, NP_001023420; SAD-1, NP_510253; *Drosophila melanogaster* PAR-1, AAF69801; CG6114 (SAD-1), NP_648814; *S. pombe* kin1, P22987.

Plasmid construction and transgenic strains

To generate the *pig-1* transcriptional fusion (*Ppig-1::gfp*), we amplified the intergenic region between *pig-1* and the nearest upstream gene, and cloned the product into the GFP vector pPD95.77 (A. Fire, S. Xu, J. Ahnn and G. Seydoux, personal communication). *gmEx320* and *gmEx321* were generated by injecting *pPD95.77*::*Ppig-1* (50 ng/μl) and the co-injection marker pRF4 [*rol-6(d)*; 50 ng/μl] (Mello et al., 1991) into N2 hermaphrodites.

To generate the *pig-1* translational fusion (*Ppig-1::pig-1::gfp)*, we amplified a full-length *pig-1* cDNA from plasmid yk400B12 and cloned the product between the *pig-1* promoter region and GFP coding sequences. *gmEx326* was generated by injecting this plasmid into N2 hermaphrodites at 50 ng/μl with 50 ng/μl pRF4.

The *Pmab-5::pig-1::gfp* construct was generated by ligating a full-length *pig-1* cDNA into plasmid *pPD95.77::Pmab-5*. pPD95.77::*Pmab-5* contains the entire *mab-5* promoter driving expression of GFP (Fleming et al., 2005). *gmEx394*, *gmEx395* and *gmEx396* were generated by injecting this plasmid into *zdIs5; pig-1(gm344)* hermaphrodites at 10 ng/μl with 50 ng/μl of pRF4 and 50 ng/μl of plasmid *Pdpy-30::NLS::DsRed2*.

The *Pdpy-30::NLS::DsRed2* plasmid was constructed by first amplifying the *dpy-30* promoter from plasmid pTY1003 (a gift from Barbara Meyer, University of California, Berkeley, CA, USA) using a reverse primer that contained a start codon followed by the SV40 T antigen nuclear localization signal (NLS) (Kalderon et al., 1984). This product was cloned into vector *pPD95.75::DsRed2* (Bulow et al., 2004).

Analysis of neuroblast daughter size

The daughters of the HSN/PHB neuroblast were identified using *gmIs20*, a nuclear-localized translational fusion between *hlh-14* and GFP (Frank et al., 2003). The size of nuclei in these cells is proportional to cell size: these cells have very little cytoplasm and are roughly spherical (Frank et al., 2005). Nuclear diameter was calculated by averaging the length of the long axis of a nucleus with the length of the perpendicular axis of the same nucleus.

The daughters of the Q.p neuroblast were identified using *ayIs9* (*Pegl-17::gfp*) (Branda and Stern, 2000). We measured cell area in a single plane of focus. These cells are extremely flat, and thus measurements of cell area are good approximations of cell size. We calculated cell area by circumscribing the cell and measuring its interior area with Openlab software (Improvision). We averaged two measurements per cell.

RESULTS

Isolation and initial characterization of *pig-1* mutants

To identify molecules that regulate asymmetric neuroblast divisions in *C. elegans*, we screened for mutants with defective asymmetric division of the HSN/PHB neuroblast. In wild-type embryos, the bilaterally symmetric HSN/PHB neuroblast divides to produce a smaller anterior daughter that undergoes programmed cell death and a larger posterior daughter, the HSN/PHB precursor (Fig. 1D). Each precursor subsequently divides to produce an HSN, a serotonergic motoneuron that stimulates egg laying by the hermaphrodite, and a PHB, a chemosensory neuron. The primary goal of our screen was to identify mutations that transform one neuroblast daughter into the other, and thereby alter the number of HSN and PHB neurons produced.

We screened for mutants with abnormal numbers of PHBs using the reporter *gmIs12*, which expresses GFP in two neurons in the tail: PHA and PHB (Hawkins et al., 2005; Troemel et al., 1995). Three maternal-effect recessive alleles of *pig-1* were isolated in these screens: *gm280*, *gm300* and *gm301*. A deletion allele, *gm344*, was subsequently isolated using a reverse-genetic approach. These mutants are relatively healthy but have a low penetrance of extra *gmIs12*-positive cells in the tail that we determined were extra PHB neurons by using PHA- or PHB-specific GFP reporters (Fig. 1G,H; Fig. 2A,B). If the extra PHB phenotype of *pig-1* mutants resulted from the production of an extra HSN/PHB precursor, *pig-1* mutants should also produce a low frequency of extra HSNs. Staining *pig-1* mutants with an anti-serotonin antibody verified this prediction (Fig. 1E,F; Fig. 2A).

Could *pig-1* act prior to the birth of the HSN/PHB neuroblast to regulate the production of HSNs and PHBs? The transcription factor *hlh-14*, for example, specifies the fate of the progenitor that generates the HSN/PHB neuroblast and its sister the PVQ neuroblast (Fig. 1B). In *hlh-14* mutants, the HSN, PHB and PVQ neurons are lost (Frank et al., 2003). We reasoned that *pig-1* mutant lineages would produce extra PVQs if the progenitor that produces the HSN/PHB and PVQ neuroblasts were duplicated, or fewer PVQs if the PVQ neuroblast were transformed into its sister, the HSN/PHB neuroblast. Using the PVQ-specific GFP reporter *kyIs39* [*Psra-6::gfp*] (Troemel et al., 1995), we scored the number of PVQs in *pig-1* mutants and found no deviation from wild type [*pig-1(gm280)*, n=138; *pig-1(gm301)*, n=118]. These observations suggest that the extra HSNs and PHBs in *pig-1* mutants arise because of defects in the HSN/PHB neuroblast or its descendants and not because of earlier lineage defects. The data are consistent with a model where *pig-1* mutations transform the anterior daughter of the HSN/PHB neuroblast, which is normally destined to die, into a second HSN/PHB precursor.

pig-1 mutants have extra neurons derived from other lineages

To address whether *pig-1* mutations perturb other lineages, we scored the number of cells produced using cell-specific GFP reporters and identified six lineages that produce extra neurons in *pig-1* mutants: the HSN/PHB, I2, M4 and PLM/ALN precursors divide during embryogenesis, and the Q.a and Q.p precursors divide during the first larval stage (Fig. 1, Fig. 2A, Fig. 3). Many other

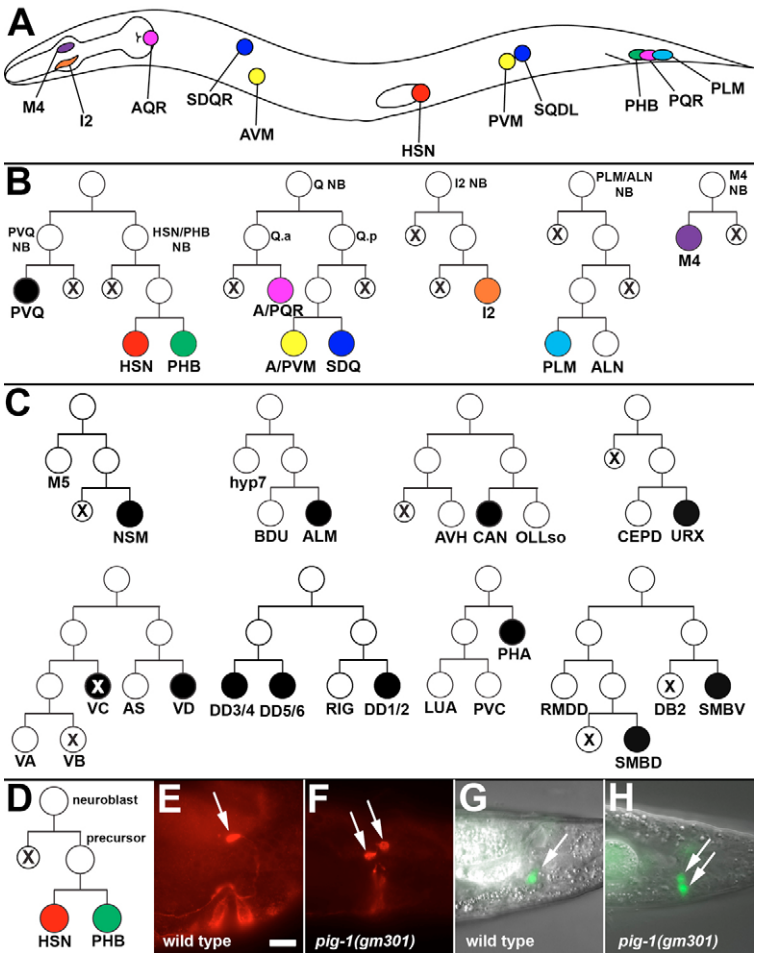

Fig. 1. *pig-1* mutants have extra neurons derived from multiple lineages. (**A**) Schematic diagram of an L1 hermaphrodite: anterior to the left, dorsal up. Neurons produced from lineages affected in *pig-1* mutants are indicated. (**B**) Lineages affected in *pig-1* mutants. NB, neuroblast. PQR, PVM and SDQL are produced by the left Q neuroblast, and AQR, AVM and SDQR are produced by the right Q neuroblast. Note that the PVQ lineage is not affected in *pig-1* mutants but is shown to indicate its relationship to the HSN/PHB lineage. (**C**) Lineages unaffected in *pig-1* mutants. Neurons that were examined are shaded black. DD1,3,5 are produced on the left side of the body, and DD2,4,6 on the right. (B,C) Neurons were identified as described in the Materials and methods. Cells that were not scored are unshaded. (**D-H**) *pig-1* mutants have extra neurons derived from the HSN/PHB neuroblast lineage. (D) Schematic diagram of the wild-type HSN/PHB neuroblast lineage. (E,F) Images of wild-type (E) and *pig-1(gm301)* (F) hermaphrodites stained with an anti-serotonin antiserum to visualize the HSNs (arrows). (G,H) Composite fluorescence and DIC images of wild-type (G) and *pig-1(gm301)* (H) hermaphrodites expressing the PHB-specific reporter *gmIs22* [*nlp-1::gfp*] (arrows). Scale bar: 10 μm.

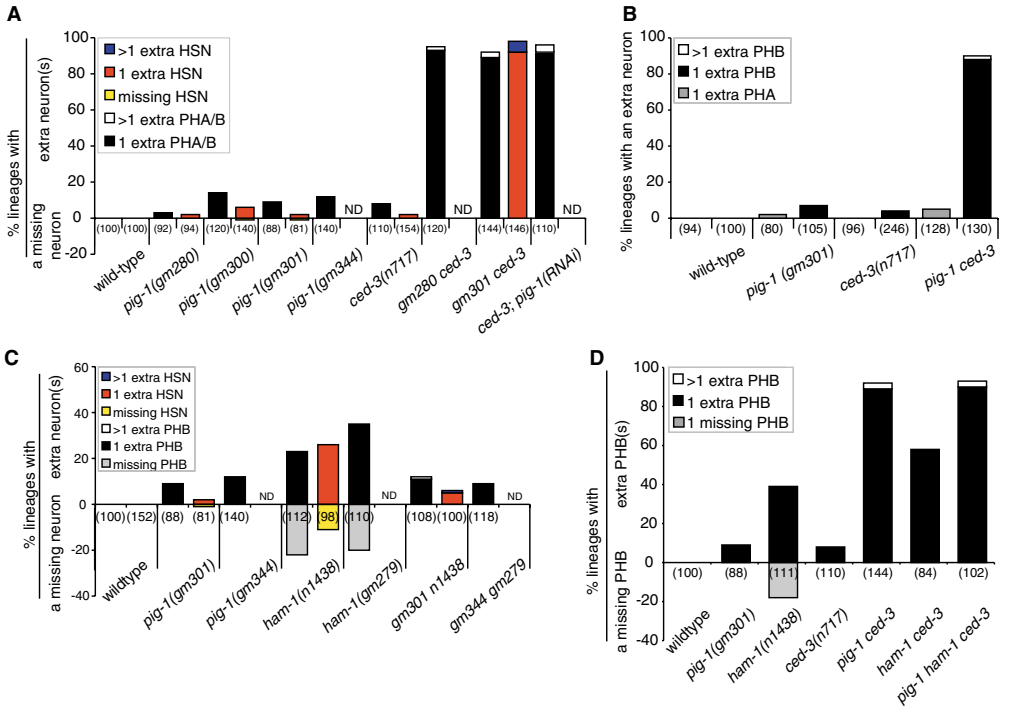

Fig. 2. *pig-1*, *ced-3* and *ham-1* HSN and PHB phenotypes. (**A**) *pig-1* mutants have extra phasmid (PHA or PHB) neurons and extra HSNs. Mutations in *pig-1* interact synergistically with mutations in *ced-3* to control the penetrance of extra neurons. The number of PHA/Bs was scored using the integrated reporter *gmIs12* [*srb-6::gfp*], and the number of HSNs was scored by immunostaining with an anti-serotonin antiserum. (**B**) The extra phasmid neurons in *pig-1* mutants are PHBs. The numbers of PHA and PHB neurons were determined using the reporters *gmIs22*[*nlp-1::gfp*] and *ynIs45*[*flp-15::gfp*], respectively. (**C**) Mutations in *pig-1* are epistatic to *ham-1*. (**D**) *pig-1* is epistatic to *ham-1* in a *ced-3* background. (C,D) The numbers of HSNs and PHBs were scored as described in A. For all genotypes, the number of lineages scored is shown below the histogram in parentheses.

lineages appear to be unaffected (Fig. 1C). The only feature shared by the affected lineages is the presence of an apoptotic cell. Our observations are consistent with a model where mutations in *pig-1* transform these cells into their sisters.

pig-1 regulates cell fate independent of the canonical programmed cell death pathway

The core programmed cell death machinery in *C. elegans* consists of four conserved proteins: EGL-1, CED-9, CED-4 and CED-3 (for reviews, see Conradt and Xue, 2005; Kaufmann and Hengartner, 2001). In wild-type animals, the BCL2-like protein CED-9 sequesters the Apaf1-like protein CED-4 to mitochondria, preventing it from interacting with the caspase CED-3. Somatic cells that undergo programmed cell death express the BH3-domain protein EGL-1. EGL-1 binds to CED-9, resulting in the release of CED-4 from mitochondria and CED-3 activation.

Two observations suggested that *pig-1* could be a component of the programmed cell death pathway. First, the low frequency of extra HSNs and PHBs observed in *pig-1* mutants closely approximates that observed in *ced-3* and *ced-4* mutants (Guenther and Garriga, 1996). Second, all of the lineages affected by *pig-1* mutations produce apoptotic cells. We hypothesized that if *pig-1* acted in a linear pathway with *ced-3*, animals with mutations in both *pig-1* and *ced-3* would have the same phenotype as the single mutants. Alternatively, if *pig-1* and *ced-3* acted in parallel, then the double mutant would have a stronger phenotype than the individual single mutants. We found that *pig-1 ced-3* double mutants had a dramatically stronger phenotype than either single mutant, resulting in nearly 100% of lineages producing extra HSNs and PHBs (Fig. 2A,B). Synergistic interactions between mutations in *pig-1* and *ced-3* were also observed in three other lineages (Q.p, I2 and PLM/ALN) that we analyzed (Fig. 3A,C,D). *pig-1* mutations also interacted synergistically with a loss-of-function mutation in *egl-1* in the Q.p and PLM lineages (Fig. 3A,D). Together, these data indicate that *pig-1* acts at least partly in parallel to the cell death pathway. Our favored interpretation of these results is that mutations in *pig-1* almost always transform the apoptotic daughter of the neuroblast into its sister, but that this transformation is usually masked by apoptosis. When this mask is removed by a mutation in a cell death gene like *ced-3*, the underlying transformation is revealed.

Lineage analysis of *pig-1*

We postulated that *pig-1* mutants have extra neurons because the cells normally fated to die in affected lineages occasionally survive and are transformed into their sister cells. To test this hypothesis, we followed the divisions of the left Q.p neuroblast, which divides to produce a posterior cell that dies (Q.pp) and the precursor to the PVM and SDQ neurons (Fig. 1B). In four out of seven Q.p divisions that we followed in *pig-1(gm344)* larvae, both neuroblast daughters survived and divided to produce two extra neurons. Because we followed the divisions in *zdIs5* [*mec-4::gfp*]*; pig-1* mutants, we determined whether the lineages that we followed produced extra PVM neurons. There was a perfect correlation between the ability of Q.pp to survive and divide and the presence of extra PVMs. In the four divisions where Q.pp survived and divided, the lineage produced an extra PVM. In the three divisions where Q.pp died, the lineage produced a single PVM. We also noted that the sizes of the *pig-1* Q.p daughter nuclei were similar, which is different from wild type where the Q.pp nucleus is much smaller than the Q.pa nucleus.

To verify that the ectopic divisions of the surviving cells in *pig-1* mutants could not be explained merely by defective apoptosis, we followed the divisions of six Q.p neuroblasts in *zdIs5; ced-3* mutants. In all of these lineages, Q.pp survived but did not divide, and none produced an extra AVM or PVM. As in wild type, the *ced-3* Q.p division was highly asymmetric, producing a large Q.pa nucleus and a small Q.pp nucleus. These observations are consistent with previous analyses of the Ced-3 phenotype in other lineages (Ellis and Horvitz, 1986; Guenther and Garriga, 1996). Together, they indicate that the apoptotic daughters of neuroblasts have different fates than their sisters, independent of their ability to survive. These data support the model that the extra neurons

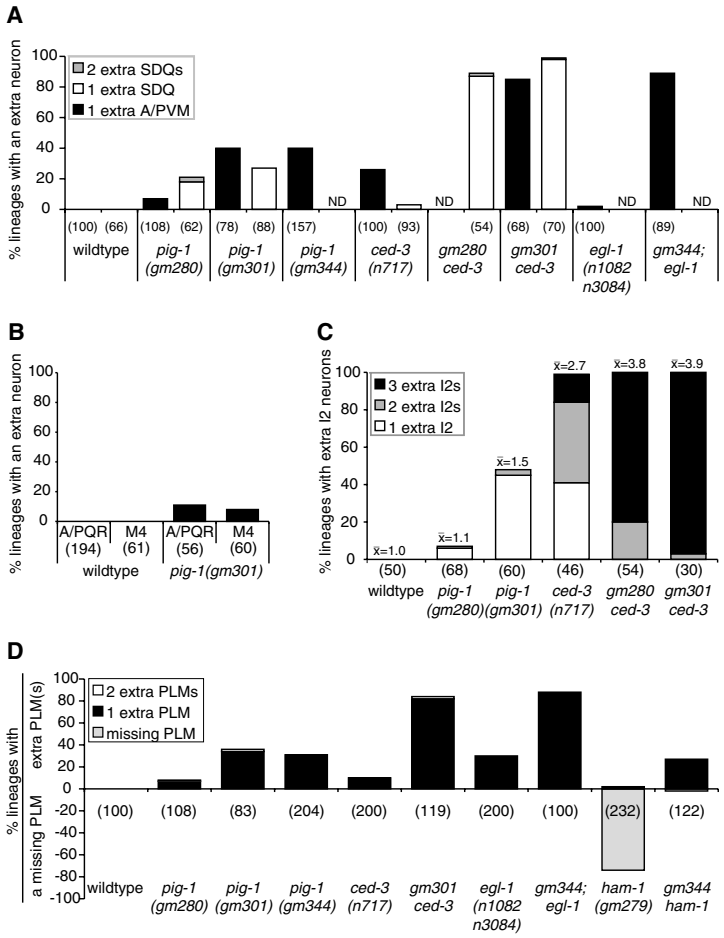

Fig. 3. *pig-1* regulates additional neuroblast lineages. (**A-D**) Neurons were identified as described in the Materials and methods. The number of lineages scored per genotype is shown in parentheses; ND, not determined. (A) *pig-1* mutants have extra AVM, PVM and SDQ neurons, all descendants of the Q.p neuroblast. (B) *pig-1* mutants have extra AQR and PQR neurons, and extra M4 neurons. (C) *pig-1* mutants have extra I2 neurons. The average number of I2 neurons per lineage is shown above the bars of the histogram. (D) *pig-1* mutants have extra PLMs and mutations in *pig-1* are epistatic to mutations in *ham-1*. As in the HSN/PHB lineage, mutations in *pig-1* interact synergistically with mutations in the pro-apoptotic genes *ced-3* and *egl-1* to control the penetrance of extra neurons in the Q.p (A), I2 (C) and PLM/ALN (D) lineages. (We did not examine *pig-1* interactions with *ced-3* or *egl-1* in the lineages that produce the A/PQR and M4 neurons.)

observed in *pig-1* mutants were generated by the inappropriate survival and transformation of cells that normally die into their sisters.

pig-1 regulates neuroblast daughter cell size asymmetry

The similar sizes of the Q.p daughter nuclei in *pig-1* mutants suggested that *pig-1* regulates the asymmetric division of neuroblasts into daughters of unequal size. To confirm a role for *pig-1* in regulating cell size, we quantified daughter cell size for both the HSN/PHB and Q.p neuroblast divisions. In the HSN/PHB neuroblast division, we used the *hlh-14::gfp* transgene *gmIs20* to measure the size of the neuroblast daughter nuclei (Frank et al., 2003). The HSN/PHB neuroblast normally divides to produce a smaller anterior daughter, which is destined to die, and a larger posterior HSN/PHB precursor. In wild-type embryos, the diameter of the nucleus of the anterior daughter was approximately three-quarters that of the nucleus of its sister, whereas, in *pig-1* mutants, the daughter nuclei were more equal in size (Fig. 4). The size differences between *pig-1* and wild-type HSN/PHB neuroblast daughter nuclei cannot be explained merely by inappropriate survival of the anterior daughter, as a mutation in *ced-3* has no phenotype in this assay (Fig. 4E). We also quantified the size of the Q.p neuroblast daughters using the cytoplasmic reporter *ayIs9* (*Pegl-17::gfp*) (Branda and Stern, 2000). Although the anterior daughter of Q.p (a neural precursor) is normally larger than its sister (which undergoes apoptosis), the daughters are more symmetric in size in *pig-1* mutants (Fig. 4F). Similar effects on daughter cell size were also observed in the Q.a division (data not shown). Together, these data indicate that *pig-1* controls daughter cell size in asymmetric neuroblast divisions.

PIG-1 encodes a conserved serine/threonine kinase

We mapped *pig-1* to a 500-kbp interval on *LGIV* containing approximately 100 genes. Three observations indicate that the open reading frame (ORF) W03G1.6 from this region is *pig-1*. First, we inactivated each ORF in this region using RNA-mediated interference (RNAi) (Kamath et al., 2001; Timmons and Fire, 1998). Only RNAi-mediated inactivation of W03G1.6 in *gmIs12*; *ced-3(n717)* animals induced a PHB duplication phenotype (Fig. 2A). Second, we sequenced the gene in three *pig-1* mutant strains and identified a single missense mutation for each allele (see below). Third, we generated a deletion allele of W03G1.6 and found that the mutant displayed Pig-1 phenotypes.

Sequence analysis of *pig-1* cDNAs indicates the gene transcribes a single SL1 trans-spliced mRNA that encodes a conserved serine/threonine kinase that is homologous to vertebrate MELK (Fig. 5). Like MELK family members, PIG-1 has an N-terminal kinase domain, a middle region of reduced homology, and a kinase-associated domain at its C terminus (Fig. 5B). Protein sequence comparisons indicate that PIG-1 and its vertebrate homologs form a separate subfamily of serine/threonine kinases distinct from the Kin1p, PAR-1 and SAD-1 families, indicating that PIG-1 is the *C. elegans* ortholog of MELK (Fig. 5C). We found that *gm300* and *gm301* alleles are missense mutations in the kinase domain that change conserved glycines to charged amino acids (Fig. 5B). The

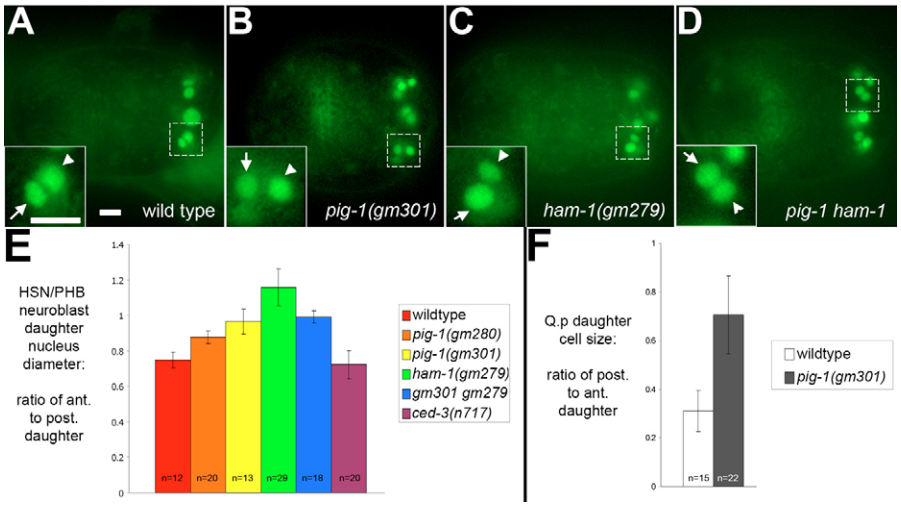

Fig. 4. *pig-1* regulates the positioning of the cleavage plane in the HSB/PHB and Q.p neuroblasts. (**A-E**) *pig-1* disrupts the size asymmetry of the daughters of the HSN/PHB neuroblast. The nuclear-localized reporter *gmIs20* (*hlh-14::gfp*) was used to identify the daughters of the HSN/PHB neuroblast and measure the size of their nuclei (Frank et al., 2005). All images show a ventral view of a single embryo with anterior to the left. In each image, the anterior (arrow) and posterior (arrowhead) daughters of the HSN/PHB neuroblast are magnified in the inset. (A) Wild type, (B) *pig-1(gm301)*, (C) *ham-1(gm279)* and (D) *pig-1(gm301) ham-1(gm279)*. Scale bars: 5 μm. (E) Quantification of the ratio in nuclear diameter between the anterior and posterior daughters of the HSN/PHB neuroblast in multiple genotypes; *n*, number of pairs of neuroblast daughters scored. (**F**) Quantification of the ratio in cell size between the posterior and anterior daughters of the Q.p neuroblast; *n*, number of pairs of neuroblast daughters scored. The transcriptional reporter *ayIs9* (*Pegl-17::gfp*) was used to identify and measure the size of the daughters of the Q.p neuroblast. Like the HSN/PHB neuroblast division, the Q.p neuroblast division is more symmetric in *pig-1* mutants.

weaker allele *gm280* is a missense mutation in the kinase-associated domain that changes a conserved glycine to arginine (Fig. 5B). This analysis indicates that both the kinase and kinase-associated domains are important for *pig-1* activity.

The *pig-1* deletion allele *gm344* is a 524 bp deletion that removes the *pig-1* promoter, all of the first exon, and part of the second exon of the *pig-1* coding sequence. *gm344* appears to be a molecular null based on RT-PCR and western blot assays (data not shown). Like the other *pig-1* mutants, *gm344* mutants are viable and the strength of Pig-1 mutant phenotypes is identical to what we observed in *pig-1(gm301)* mutants (Fig. 3A,D). These comparisons suggest that the alleles *gm300*, *gm301* and *gm344* eliminate PIG-1 function, and that the allele *gm280* reduces it.

PIG-1 expression and localization

Pig-1 phenotypes are maternally rescued, consistent with the presence of *pig-1* transcripts in the hermaphrodite germ line (NEXT database, Y. Kohara, personal communication). To characterize zygotic *pig-1* expression, we examined transgenic worms expressing a transcriptional reporter containing 850 bp upstream of the *pig-1* start codon fused to GFP coding sequences. This construct contained all of the noncoding sequence between *pig-1* and the next predicted upstream gene, and expressed GFP ubiquitously in early embryos. The expression became progressively more restricted in older embryos and young larvae, and was not observed in adults (data not shown). In larvae, we observed expression in dividing cells: ventral nerve cord neuroblasts, vulval precursors, dividing hypodermal

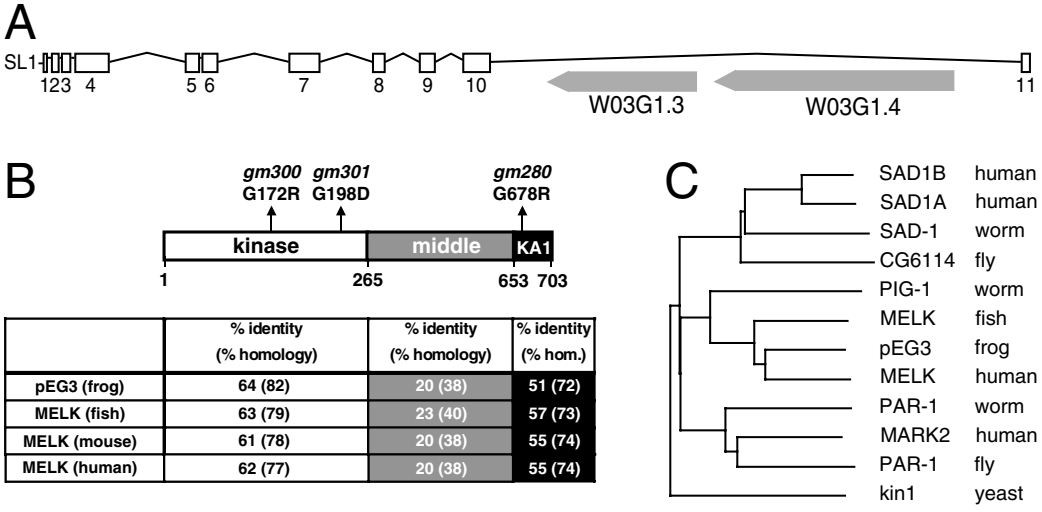

	% identity (% homology)	% identity (% homology)	% identity (% hom.)
pEG3 (frog)	64 (82)	20 (38)	51 (72)
MELK (fish)	63 (79)	23 (40)	57 (73)
MELK (mouse)	61 (78)	20 (38)	55 (74)
MELK (human)	62 (77)	20 (38)	55 (74)

Fig. 5. Molecular characterization of *pig-1*. (**A**) Schematic diagram of the *pig-1* transcript. White boxes represent exons, and the location of the SL1-splice leader is indicated. The terminal intron of *pig-1* contains two genes, depicted as grey arrows, that are transcribed in the opposite orientation to *pig-1*. (**B**) Schematic diagram of the domain architecture of the PIG-1 protein, depicting the N-terminal kinase domain (unshaded) and the C-terminal kinase-associated domain (black). The locations and identities of the *gm300*, *gm301* and *gm280* missense mutations are shown above the diagram. Below the diagram is a table comparing each domain in PIG-1 to orthologs in frog, fish, mouse and human. (**C**) Phylogenetic relationship of PIG-1 to selected members of the PAR-1/SAD-1/Kin1 superfamily of serine/threonine kinases. PIG-1 clusters with other MELK family members.

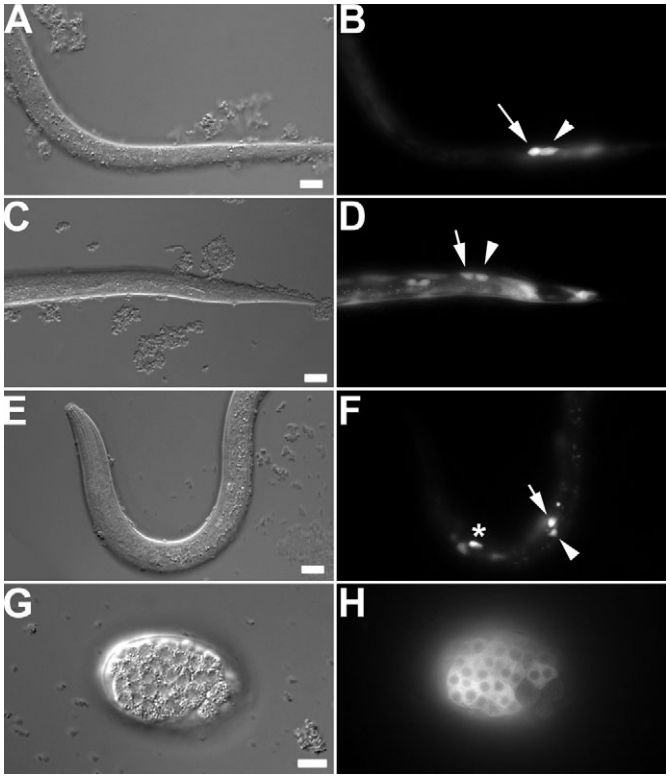

Fig. 6. Expression and subcellular localization of PIG-1. (**A-F**) Images of larvae expressing *Ppig-1::gfp*: anterior, left; ventral, up. (A,C,E) DIC microscopy; (B,D,F) GFP fluorescence. (A,B) L1 larva expressing *Ppig-1::gfp* in the Q neuroblast (arrow) and V5 seam cell (arrowhead). (C,D) L1 larva expressing *Ppig-1::gfp* in the Q neuroblast daughters Q.a (arrow) and Q.p (arrowhead). (E,F) L1 larva expressing *Ppig-1::gfp* in the Q lineage descendants AQR (asterisk), AVM (arrow), and SQDR (arrowhead). (**G**,**H**) DIC (G) and fluorescence (H) images of an embryo expressing *Ppig-1::pig-1::gfp. pig-1::gfp* is present throughout the cytoplasm and excluded from the nucleus. Scale bars: 10 μm.

seam cells, and the Q neuroblasts and their descendants (Fig. 6A-F; data not shown). To investigate the subcellular distribution of the PIG-1 protein, we examined transgenic worms expressing a full-length *pig-1::gfp* translational fusion. This construct contains the same promoter used in the transcriptional reporter fused to a full-length *pig-1* cDNA tagged with GFP. This transgene rescued Pig-1 phenotypes in the PLM/ALN and Q.p lineages (data not shown). In all cells, the fusion protein was localized to the cytoplasm and excluded from nuclei (Fig. 6G,H).

pig-1 acts cell autonomously in the Q.p lineage

To determine whether *pig-1* acts cell autonomously in neuroblasts to regulate their divisions, we focused on the Q.p neuroblast, which produces the A/PVM and SDQ neurons (Fig. 1B). The *pig-1* promoter drives expression in the Q neuroblast and its descendents (Fig. 6A-F), consistent with a cell autonomous role for *pig-1*. To test this hypothesis, we expressed a *pig-1* cDNA from the *mab-5* promoter and asked whether its expression would rescue the Q.p defects of *pig-1* mutants. *mab-5* encodes a homeobox transcription factor expressed in a bilaterally symmetric group of posterior cells with one exception: it is expressed in the left Q lineage (which produces PVM), but not the right Q lineage (which produces AVM)

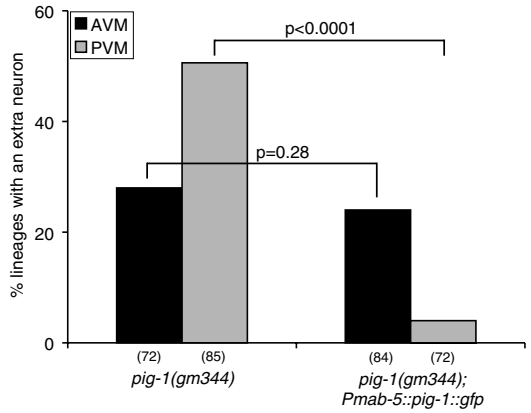

Fig. 7. PIG-1 acts cell-autonomously to regulate the asymmetric division of the Q.p neuroblast. The numbers of AVM and PVM neurons were scored using *zdls5* [*mec-4::gfp*]; the number of lineages scored is shown in parentheses. Expression of *pig-1* from the *mab-5* promoter does not rescue the extra AVM phenotype of *pig-1(gm344)* but does rescue the extra PVM phenotype. Statistical analysis was performed using a one-tailed two-sample *Z*-test (using the normal approximation to the binomial distribution) by the StatCrunch program (www.statcrunch.com).

(Cowing and Kenyon, 1992; Salser and Kenyon, 1992). We reasoned that if *pig-1* acts in the Q lineage, *pig-1* expression from the *mab-5* promoter should rescue the extra PVM but not the extra AVM phenotype of *pig-1* mutants. Consistent with the hypothesis that PIG-1 acts in Q.p to promote its asymmetric division, the *Pmab-5::pig-1* transgene rescued the Pig-1 PVM but not the AVM phenotype (Fig. 7).

pig-1 and *ham-1* genetic interactions

The *C. elegans* HAM-1 protein regulates the asymmetric divisions of many embryonic neuroblasts, including the HSN/PHB neuroblast (Frank et al., 2005; Guenther and Garriga, 1996). Like mutations in *pig-1*, mutations in *ham-1* alter both HSN/PHB neuroblast daughter cell size asymmetry and cell fate. In *ham-1(gm279)* null mutants, the relative sizes of the neuroblast daughters are reversed, and the anterior daughter is larger than its sister. The anterior daughter is transformed into its sister, resulting in the production of extra HSNs and PHBs. *ham-1* HSNs and PHBs also often fail to differentiate properly, and occasionally mutant lineages fail to produce HSNs or PHBs that express cell-type specific markers; this latter phenotype may be a consequence of the failure of the posterior daughter of the HSN/PHB neuroblast to divide or differentiate correctly because of its small size. *ham-1* encodes a novel protein that is asymmetrically distributed to the posterior cortex of the dividing neuroblast and is inherited specifically by the precursor. HAM-1 is hypothesized to control the asymmetric segregation of developmental potential into the neuroblast daughters, in part by regulating the volume of neuroblast cytoplasm distributed to each daughter cell (Frank et al., 2005).

The similarity of *pig-1* and *ham-1* phenotypes led us to determine whether the two genes act together to regulate neuroblast divisions. To address this possibility, we examined the output of the HSN/PHB neuroblast lineage in *pig-1 ham-1* double mutants. While *pig-1* mutants have a low penetrance of extra PHBs, *ham-1* mutants have a higher penetrance of extra PHBs, as well as missing PHBs (Fig. 2C). We were surprised to discover that although *ham-1* mutants have a stronger phenotype, *pig-1* mutations were epistatic to *ham-1*

mutations: *pig-1 ham-1* double mutants had a low penetrance of extra PHBs and were not missing PHBs. This relationship was observed with multiple *pig-1* and *ham-1* alleles (Fig. 2C; data not shown). We obtained similar results when we scored the number of HSNs (Fig. 2C) and the number of PLMs (Fig. 3D), indicating that the genetic interaction between the two genes is not PHB or lineage specific. Mutations in *pig-1* are also epistatic to *ham-1* in a *ced-3* background: whereas *ham-1(n1438) ced-3* double mutants have extra PHBs about 60% of the time, *pig-1 ced-3* and *pig-1 ham-1(n1438) ced-3* mutants almost always have extra cells (Fig. 2D).

pig-1 mutations also suppressed Ham-1 differentiation phenotypes. The PHB phasmid neurons in *ham-1* mutants frequently fail to fill with the dye DiI because of defective sensilla development (Guenther and Garriga, 1996). *pig-1* mutants have no dye-filling defects, and mutations in *pig-1* suppress the dye-filling defects of *ham-1* mutants (data not shown). *pig-1* mutations also suppress the HSN migration defects observed in *ham-1* mutants (data not shown).

Mutations in both *pig-1* and *ham-1* perturb the asymmetric division of the HSN/PHB neuroblast into daughters of unequal size. While strong *ham-1* mutations reverse the relative sizes of the daughters (Frank et al., 2005), mutations in *pig-1* cause the neuroblast to divide more symmetrically. When we compared the sizes of the HSN/PHB neuroblast daughters in *pig-1 ham-1* double mutants, we found that they were similar to *pig-1* mutants (Fig. 4). In summary, *pig-1 ham-1* double mutants seem to phenocopy *pig-1* single mutants in assays that examine the cell lineage, cell size, and the differentiation of neuroblast descendants in the HSN/PHB neuroblast lineage.

DISCUSSION

pig-1 may regulate neuroblast polarity

Many genes that regulate asymmetric cell divisions control cell polarity. For example, the PAR proteins are required in the *C. elegans* zygote for the asymmetric positioning of the mitotic spindle and the asymmetric segregation of cell fate determinants to daughter cells (Kemphues et al., 1988; Rose and Kemphues, 1998). *pig-1* mutants share phenotypic features with these cell polarity mutants, and PIG-1 is related molecularly to PAR-1. However, although *pig-1* and *par-1* phenotypes have similar features, PAR-1 localizes asymmetrically in the mother cell, whereas PIG-1 and its vertebrate orthologs do not (Chartrain et al., 2005; Heyer et al., 1999). The symmetric distribution of PIG-1 suggests that it may play a permissive role in the regulation of neuroblast polarity. In this sense, PIG-1 may resemble the symmetrically distributed 14-3-3 protein PAR-5, which regulates both spindle positioning and cell fate in the *C. elegans* zygote (Morton et al., 2002).

We propose that PIG-1 controls the asymmetric positioning of the mitotic spindle and asymmetric segregation of neural fate determinants to daughter cells. In this model, loss of *pig-1* activity disrupts neuroblast polarity, resulting in symmetric positioning of the cleavage plane and mislocalization of cell fate determinants. The neuroblast therefore divides symmetrically, and cell fate determinants are symmetrically distributed to daughter cells. The segregation of these determinants into the normally apoptotic daughter of the neuroblast transforms it into its sister.

HAM-1 is also thought to regulate asymmetric neuroblast divisions by regulating neuroblast polarity, and mutations in *ham-1* also disrupt cell size asymmetry and cell fate in the HSN/PHB neuroblast division. HAM-1 has previously been proposed to regulate neuroblast daughter cell fate in part by controlling cell size (Frank et al., 2005). One important question that arises from our analysis is whether HAM-1 and PIG-1 could function solely to regulate the position of the neuroblast cleavage plane, and the ensuing cell fate transformation could result from altered daughter cell size. This model predicts that determinants are symmetrically distributed in the neuroblast and that cell fate is determined by the concentration of determinants in a neuroblast daughter. Alternatively, PIG-1 and HAM-1 could regulate the position of the neuroblast cleavage plane and the asymmetric segregation of cell fate determinants to daughter cells independently. In this model, determinants are asymmetrically distributed in the neuroblast, and their segregation into daughter cells is mostly independent of cleavage plane position.

Two observations lead us to favor a modified version of the second model, in which the size of daughter cells does not directly specify their fate, but might influence their survival (Fig. 8). First, cell size alone cannot control the apoptotic fate of the daughter cells. Although the posterior daughter of the HSN/PHB neuroblast is

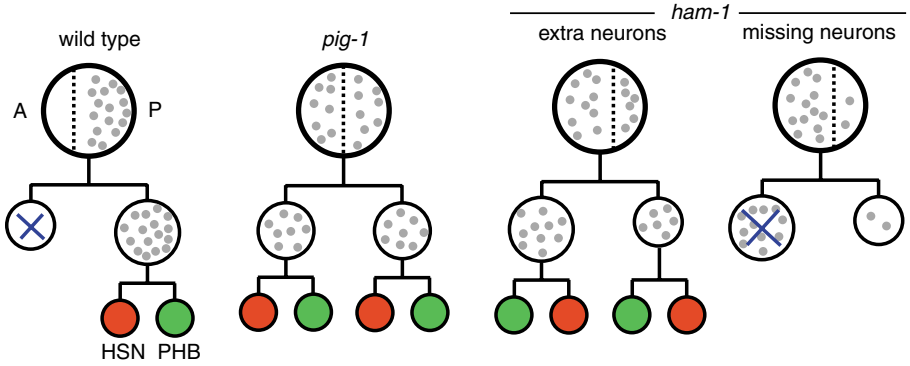

Fig. 8. Modeling the HSN/PHB lineage in *pig-1* and *ham-1* mutants. In wild-type animals, the HSN/PHB neuroblast is polarized along the AP axis, with an anteriorly displaced cleavage plane (vertical dotted line) and posteriorly localized determinants of neural precursor fate (gray circles). The neuroblast divides to produce a small anterior daughter that inherits no determinants and undergoes apoptosis, and a larger posterior daughter that inherits the determinants and becomes a neural precursor. In *pig-1* mutants, the neuroblast does not polarize and this results in a symmetrically localized cleavage plane and uniformly distributed determinants. Both neuroblast daughters inherit these determinants resulting in the production of two neural precursors. In *ham-1* mutants, neuroblast polarity is partially inverted along the AP axis resulting in a posteriorly displaced cleavage plane and an anteriorly enriched distribution of cell fate determinants. Extra neurons are produced when a sufficient concentration of determinants enters both neuroblast daughters, resulting in the production of two precursors. No neurons are produced when the anterior daughter undergoes apoptosis and the posterior daughter receives an insufficient concentration of determinants to develop as a precursor. The concentration of determinants in the posterior daughter could fall below a threshold required for precursor fate, either because of stochastic differences in cleavage position or determinant distribution. Neuroblasts in *pig-1 ham-1* double mutants are defective for polarity, resulting in *pig-1* phenotypes and *pig-1* epistasis to *ham-1*.

smaller in *ham-1* mutants, it is still the larger anterior daughter that dies (Frank et al., 2005). Second, if cleavage plane position were to regulate quantitative differences in the segregation of cell fate determinants to the anterior daughter of the HSN/PHB neuroblast, the frequency at which this cell is transformed into its sister in *pig-1* and *ham-1* mutants should be proportional to the deviation of the cleavage plane from its normal position. This does not seem to be the case, as analyses of *pig-1 ced-3* and *ham-1 ced-3* double mutants suggest that *pig-1* and *ham-1* mutations always transform the anterior daughter of the HSN/PHB neuroblast into its sister, independent of daughter cell size. However, the penetrance of extra cells in *pig-1*, *ham-1* and *pig-1 ham-1* mutants does appear to be proportional to the deviation of the cleavage plane from its normal position, so cell size could affect the frequency at which the anterior daughter of the neuroblast escapes programmed cell death. Thus, increasing the size of the anterior daughter of the HSN/PHB neuroblast may increase the frequency at which this cell escapes programmed cell death.

The epistatic interactions between the *pig-1* and *ham-1* mutations are intriguing. If daughter cell size influences the penetrance of extra and missing neurons, then *pig-1*'s epistasis to *ham-1* at the level of daughter size is sufficient to explain why *pig-1* mutations suppress the extra neuron and missing neuron phenotypes of *ham-1* mutants (Fig. 8). *pig-1* might be epistatic to *ham-1* because HAM-1 inhibits PIG-1-dependent positioning of the mitotic spindle. HAM-1 may restrict PIG-1 activity to the anterior of the HSN/PHB neuroblast, and the mispositioning of the cleavage plane in *ham-1* mutants could be a consequence of ectopic PIG-1 activity in the posterior of the neuroblast. Alternatively, PIG-1 might be a general factor required for spindle positioning. PIG-1, for example, could regulate, or be regulated by, both HAM-1 and an activity that has been postulated to antagonize HAM-1 (Frank et al., 2005).

PIG-1 and MELK

The vertebrate orthologs of PIG-1 have been implicated in regulating cell proliferation, although the nature of this regulation has been the subject of debate. MELK kinase activity exhibits cell cycle dependence, with maximal activity during mitosis (Blot et al., 2002; Davezac et al., 2002). MELK has been shown to bind and phosphorylate CDC25B, a phosphatase that promotes G2/M progression by removing inhibitory phosphate groups from the cyclin-dependent kinase CDC2 (Davezac et al., 2002). MELK phosphorylation was proposed to inhibit CDC25B, as several groups have shown that MELK overexpression results in a block at the G2/M boundary (Davezac et al., 2002; Gray et al., 2005; Vulsteke et al., 2004). The *C. elegans* genome encodes three CDC25 homologs. To determine whether Pig-1 phenotypes require CDC-25 activity, we used RNAi (Fraser et al., 2000) to inactivate these genes in *pig-1* and *pig-1 ced-3* animals. We examined the output of the HSN/PHB and PLM/ALN lineages, and found that RNAi of *cdc-25.2* suppressed the extra PHB and PLM phenotypes of these mutants (A. Singhvi and G.G., unpublished). While these observations are consistent with a role for PIG-1 as a negative regulator of CDC-25.2, it is also possible that the *cdc-25.2* RNAi effects reflect a nonspecific effect on cell division.

MELK has also been proposed to positively regulate the cell cycle. Overexpression of MELK in mouse neurosphere cultures results in increased proliferation, whereas MELK knockdown by siRNA has the opposite effect (Nakano et al., 2005). MELK has also been shown to positively regulate the growth rate of cultured human tumor cell lines, both in vitro and after injection into a murine host (Gray et al., 2005). Nakano et al. (Nakano et al., 2005) proposed that MELK positively regulates the cell cycle through its association with the zinc-finger protein ZPR9 and the proto-oncogene B-myb. MELK binds and phosphorylates ZPR9 (Seong et al., 2002), which in turn binds B-myb and increases its transcriptional activity (Seong et al., 2003). Although an ortholog of ZPR9 exists in *C. elegans* (ORF C16A3.4), RNAi of this gene does not generate a Pig-1-like phenotype (S.C. and G.G., unpublished).

Altered cell cycle progression in the neuroblast could lead to the phenotypes observed in *pig-1* mutants, as cell cycle regulators are known to control asymmetric divisions. In *Drosophila*, Cdc2/B type cyclins regulate asymmetric divisions of neuroblasts in the central nervous system. Loss of zygotic *cdc2* activity results in both defective spindle positioning and sister-sister cell fate transformations (Tio et al., 2001). In *C. elegans*, the anaphase-promoting complex (APC), the APC activator *cdc20* and the APC effector separin are required during the first cell division for proper positioning of the cleavage plane and the asymmetric distribution of cell fate determinants (Rappleye et al., 2002). PIG-1 could regulate the timing of cell cycle events in the neuroblast, which in turn, could indirectly regulate neuroblast polarity. In conclusion, our analysis of PIG-1 suggests that MELK could regulate polarity and daughter cell fate in asymmetrically dividing cell lineages such as stem cells.

We thank A. Singhvi and N. Hawkins for comments on the manuscript, A. Singhvi for sharing unpublished observations, and members of the Garriga, Meyer and Dernburg labs for helpful discussions. We also thank Y. Kohara for cDNAs and C. Li, Y. Lie, C. Kenyon, O. Hobert and B. Meyer for bacterial and *C. elegans* strains. Some of the *C. elegans* strains used in this study were obtained from the *C. elegans* Genetics Center, which is funded by the NIH National Center for Research Resources. This work was supported by an Ernest Brown Babcock Scholarship to S.C., a National Science Foundation predoctoral fellowship to C.A.F., and by National Institutes of Health grant NS42213 to G.G.

References

Blot, J., Chartrain, I., Roghi, C., Philippe, M. and Tassan, J. P. (2002). Cell cycle regulation of pEg3, a new Xenopus protein kinase of the KIN1/PAR-1/MARK family. *Dev. Biol.* **241**, 327-338.

Branda, C. S. and Stern, M. J. (2000). Mechanisms controlling sex myoblast migration in Caenorhabditis elegans hermaphrodites. *Dev. Biol.* **226**, 137-151.

Brenner, S. (1974). The genetics of Caenorhabditis elegans. *Genetics* **77**, 71-94.

Bulow, H. E., Boulin, T. and Hobert, O. (2004). Differential functions of the C. elegans FGF receptor in axon outgrowth and maintenance of axon position. *Neuron* **42**, 367-374.

Chartrain, I., Couturier, A. and Tassan, J. P. (2005). Cell cycle dependent cortical localization of pEg3 protein kinase in Xenopus and human cells. *Biol. Cell.* **98**, 253-263.

Clark, S. G. and Chiu, C. (2003). C. elegans ZAG-1, a Zn-finger-homeodomain protein, regulates axonal development and neuronal differentiation. *Development* **130**, 3781-3794.

Cohen, D., Brennwald, P. J., Rodriguez-Boulan, E. and Musch, A. (2004). Mammalian PAR-1 determines epithelial lumen polarity by organizing the microtubule cytoskeleton. *J. Cell Biol.* **164**, 717-727.

Conradt, B. and Horvitz, H. R. (1998). The C. elegans protein EGL-1 is required for programmed cell death and interacts with the Bcl-2-like protein CED-9. *Cell* **93**, 519-529.

Conradt, B. and Xue, D. (2005). Programmed cell death. In *Wormbook* (ed. The C. elegans Research Community). http://www.wormbook.org, doi/10.1895/wormbook.1.32.1.

Cowing, D. W. and Kenyon, C. (1992). Expression of the homeotic gene mab-5 during Caenorhabditis elegans embryogenesis. *Development* **116**, 481-490.

Cox, D. N., Lu, B., Sun, T. Q., Williams, L. T. and Jan, Y. N. (2001). Drosophila par-1 is required for oocyte differentiation and microtubule organization. *Curr. Biol.* **11**, 75-87.

Crump, J. G., Zhen, M., Jin, Y. and Bargmann, C. I. (2001). The SAD-1 kinase regulates presynaptic vesicle clustering and axon termination. *Neuron* **29**, 115-129.

Davezac, N., Baldin, V., Blot, J., Ducommun, B. and Tassan, J. P. (2002). Human pEg3 kinase associates with and phosphorylates CDC25B phosphatase: a potential role for pEg3 in cell cycle regulation. *Oncogene* **21**, 7630-7641.

Desai, C., Garriga, G., McIntire, S. L. and Horvitz, H. R. (1988). A genetic pathway for the development of the Caenorhabditis elegans HSN motor neurons. *Nature* **336**, 638-646.

Doerflinger, H., Benton, R., Shulman, J. M. and St Johnston, D. (2003). The role of PAR-1 in regulating the polarised microtubule cytoskeleton in the Drosophila follicular epithelium. *Development* **130**, 3965-3975.
Drewes, G. and Nurse, P. (2003). The protein kinase kin1, the fission yeast orthologue of mammalian MARK/PAR-1, localises to new cell ends after mitosis and is important for bipolar growth. *FEBS Lett.* **554**, 45-49.
Easterday, M. C., Dougherty, J. D., Jackson, R. L., Ou, J., Nakano, I., Paucar, A. A., Roobini, B., Dianati, M., Irvin, D. K., Weissman, I. L. et al. (2003). Neural progenitor genes. Germinal zone expression and analysis of genetic overlap in stem cell populations. *Dev. Biol.* **264**, 309-322.
Ellis, H. M. and Horvitz, H. R. (1986). Genetic control of programmed cell death in the nematode C. elegans. *Cell* **44**, 817-829.
Fleming, T. C., Wolf, F. W. and Garriga, G. (2005). Sensitized genetic backgrounds reveal a role for C. elegans FGF EGL-17 as a repellent for migrating CAN neurons. *Development* **132**, 4857-4867.
Frank, C. A., Baum, P. D. and Garriga, G. (2003). HLH-14 is a C. elegans Achaete-Scute protein that promotes neurogenesis through asymmetric cell division. *Development* **130**, 6507-6518.
Frank, C. A., Hawkins, N. C., Guenther, C., Horvitz, H. R. and Garriga, G. (2005). C. elegans HAM-1 positions the cleavage plane and regulates apoptosis in asymmetric neuroblast divisions. *Dev. Biol.* **284**, 301-310.
Fraser, A. G., Kamath, R. S., Zipperlen, P., Martinez-Campos, M., Sohrmann, M. and Ahringer, J. (2000). Functional genomic analysis of C. elegans chromosome I by systematic RNA interference. *Nature* **408**, 325-330.
Garriga, G., Desai, C. and Horvitz, H. R. (1993). Cell interactions control the direction of outgrowth, branching and fasciculation of the HSN axons of Caenorhabditis elegans. *Development* **117**, 1071-1087.
Gil, M., Yang, Y., Lee, Y., Choi, I. and Ha, H. (1997). Cloning and expression of a cDNA encoding a novel protein serine/threonine kinase predominantly expressed in hematopoietic cells. *Gene* **195**, 295-301.
Gray, D., Jubb, A. M., Hogue, D., Dowd, P., Kljavin, N., Yi, S., Bai, W., Frantz, G., Zhang, Z., Koeppen, H. et al. (2005). Maternal embryonic leucine zipper kinase/murine protein serine-threonine kinase 38 is a promising therapeutic target for multiple cancers. *Cancer Res.* **65**, 9751-9761.
Guenther, C. and Garriga, G. (1996). Asymmetric distribution of the C. elegans HAM-1 protein in neuroblasts enables daughter cells to adopt distinct fates. *Development* **122**, 3509-3518.
Guo, S. and Kemphues, K. J. (1995). par-1, a gene required for establishing polarity in C. elegans embryos, encodes a putative Ser/Thr kinase that is asymmetrically distributed. *Cell* **81**, 611-620.
Hawkins, N. C., Ellis, G. C., Bowerman, B. and Garriga, G. (2005). MOM-5 Frizzled regulates the distribution of DSH-2 to control C. elegans asymmetric neuroblast divisions. *Dev. Biol.* **284**, 246-259.
Hedgecock, E. M., Culotti, J. G., Hall, D. H. and Stern, B. D. (1987). Genetics of cell and axon migrations in Caenorhabditis elegans. *Development* **100**, 365-382.
Heyer, B. S., Warsowe, J., Solter, D., Knowles, B. B. and Ackerman, S. L. (1997). New member of the Snf1/AMPK kinase family, Melk, is expressed in the mouse egg and preimplantation embryo. *Mol. Reprod. Dev.* **47**, 148-156.
Heyer, B. S., Kochanowski, H. and Solter, D. (1999). Expression of Melk, a new protein kinase, during early mouse development. *Dev. Dyn.* **215**, 344-351.
Hobert, O., D'Alberti, T., Liu, Y. and Ruvkun, G. (1998). Control of neural development and function in a thermoregulatory network by the LIM homeobox gene lin-11. *J. Neurosci.* **18**, 2084-2096.
Horvitz, H. R. and Herskowitz, I. (1992). Mechanisms of asymmetric cell division: two Bs or not two Bs, that is the question. *Cell* **68**, 237-255.
Jin, Y., Jorgensen, E., Hartwieg, E. and Horvitz, H. R. (1999). The Caenorhabditis elegans gene unc-25 encodes glutamic acid decarboxylase and is required for synaptic transmission but not synaptic development. *J. Neurosci.* **19**, 539-548.
Kalderon, D., Roberts, B. L., Richardson, W. D. and Smith, A. E. (1984). A short amino acid sequence able to specify nuclear location. *Cell* **39**, 499-509.
Kamath, R. S., Martinez-Campos, M., Zipperlen, P., Fraser, A. G. and Ahringer, J. (2001). Effectiveness of specific RNA-mediated interference through ingested double-stranded RNA in Caenorhabditis elegans. *Genome Biol.* **2**, RESEARCH0002.
Kaufmann, S. H. and Hengartner, M. O. (2001). Programmed cell death: alive and well in the new millennium. *Trends Cell. Biol.* **11**, 526-534.
Kemphues, K. J., Priess, J. R., Morton, D. G. and Cheng, N. S. (1988). Identification of genes required for cytoplasmic localization in early C. elegans embryos. *Cell* **52**, 311-320.
Kim, K. and Li, C. (2004). Expression and regulation of an FMRFamide-related neuropeptide gene family in Caenorhabditis elegans. *J. Comp. Neurol.* **475**, 540-550.
Kishi, M., Pan, Y. A., Crump, J. G. and Sanes, J. R. (2005). Mammalian SAD kinases are required for neuronal polarization. *Science* **307**, 929-932.
La Carbona, S., Allix, C., Philippe, M. and Le Goff, X. (2004). The protein kinase kin1 is required for cellular symmetry in fission yeast. *Biol. Cell* **96**, 169-179.
Li, C., Kim, K. and Nelson, L. S. (1999a). FMRFamide-related neuropeptide gene family in Caenorhabditis elegans. *Brain Res.* **848**, 26-34.
Li, C., Nelson, L. S., Kim, K., Nathoo, A. and Hart, A. C. (1999b). Neuropeptide gene families in the nematode Caenorhabditis elegans. *Ann. N. Y. Acad. Sci.* **897**, 239-252.
Mello, C. C., Kramer, J. M., Stinchcomb, D. and Ambros, V. (1991). Efficient gene transfer in C.elegans: extrachromosomal maintenance and integration of transforming sequences. *EMBO J.* **10**, 3959-3970.
Morton, D. G., Shakes, D. C., Nugent, S., Dichoso, D., Wang, W., Golden, A. and Kemphues, K. J. (2002). The Caenorhabditis elegans par-5 gene encodes a 14-3-3 protein required for cellular asymmetry in the early embryo. *Dev. Biol.* **241**, 47-58.
Nakano, I., Paucar, A. A., Bajpai, R., Dougherty, J. D., Zewail, A., Kelly, T. K., Kim, K. J., Ou, J., Groszer, M., Imura, T. et al. (2005). Maternal embryonic leucine zipper kinase (MELK) regulates multipotent neural progenitor proliferation. *J. Cell Biol.* **170**, 413-427.
Perriere, G. and Gouy, M. (1996). WWW-query: an on-line retrieval system for biological sequence banks. *Biochimie* **78**, 364-369.
Rappleye, C. A., Tagawa, A., Lyczak, R., Bowerman, B. and Aroian, R. V. (2002). The anaphase-promoting complex and separin are required for embryonic anterior-posterior axis formation. *Dev. Cell* **2**, 195-206.
Rose, L. S. and Kemphues, K. J. (1998). Early patterning of the C. elegans embryo. *Annu. Rev. Genet.* **32**, 521-545.
Saito, R., Tabata, Y., Muto, A., Arai, K. and Watanabe, S. (2005). Melk-like kinase plays a role in hematopoiesis in the zebra fish. *Mol. Cell. Biol.* **25**, 6682-6693.
Salser, S. J. and Kenyon, C. (1992). Activation of a C. elegans Antennapedia homologue in migrating cells controls their direction of migration. *Nature* **355**, 255-258.
Seong, H. A., Gil, M., Kim, K. T., Kim, S. J. and Ha, H. (2002). Phosphorylation of a novel zinc-finger-like protein, ZPR9, by murine protein serine/threonine kinase 38 (MPK38). *Biochem. J.* **361**, 597-604.
Seong, H. A., Kim, K. T. and Ha, H. (2003). Enhancement of B-MYB transcriptional activity by ZPR9, a novel zinc finger protein. *J. Biol. Chem.* **278**, 9655-9662.
Shulman, J. M., Benton, R. and St Johnston, D. (2000). The Drosophila homolog of C. elegans PAR-1 organizes the oocyte cytoskeleton and directs oskar mRNA localization to the posterior pole. *Cell* **101**, 377-388.
Simmer, F., Tijsterman, M., Parrish, S., Koushika, S. P., Nonet, M. L., Fire, A., Ahringer, J. and Plasterk, R. H. (2002). Loss of the putative RNA-directed RNA polymerase RRF-3 makes C. elegans hypersensitive to RNAi. *Curr. Biol.* **12**, 1317-1319.
Sulston, J. E. and Horvitz, H. R. (1977). Post-embryonic cell lineages of the nematode, Caenorhabditis elegans. *Dev. Biol.* **56**, 110-156.
Thompson, J. D., Gibson, T. J., Plewniak, F., Jeanmougin, F. and Higgins, D. G. (1997). The CLUSTAL_X windows interface: flexible strategies for multiple sequence alignment aided by quality analysis tools. *Nucleic Acids Res.* **25**, 4876-4882.
Timmons, L. and Fire, A. (1998). Specific interference by ingested dsRNA. *Nature* **395**, 854.
Tio, M., Udolph, G., Yang, X. and Chia, W. (2001). cdc2 links the Drosophila cell cycle and asymmetric division machineries. *Nature* **409**, 1063-1067.
Tomancak, P., Piano, F., Riechmann, V., Gunsalus, K. C., Kemphues, K. J. and Ephrussi, A. (2000). A Drosophila melanogaster homologue of Caenorhabditis elegans par-1 acts at an early step in embryonic-axis formation. *Nat. Cell Biol.* **2**, 458-460.
Troemel, E. R., Chou, J. H., Dwyer, N. D., Colbert, H. A. and Bargmann, C. I. (1995). Divergent seven transmembrane receptors are candidate chemosensory receptors in C. elegans. *Cell* **83**, 207-218.
Vulsteke, V., Beullens, M., Boudrez, A., Keppens, S., Van Eynde, A., Rider, M. H., Stalmans, W. and Bollen, M. (2004). Inhibition of spliceosome assembly by the cell cycle-regulated protein kinase MELK and involvement of splicing factor NIPP1. *J. Biol. Chem.* **279**, 8642-8647.
Wicks, S. R., Yeh, R. T., Gish, W. R., Waterston, R. H. and Plasterk, R. H. (2001). Rapid gene mapping in Caenorhabditis elegans using a high density polymorphism map. *Nat. Genet.* **28**, 160-164.
Withee, J., Galligan, B., Hawkins, N. and Garriga, G. (2004). Caenorhabditis elegans WASP and Ena/VASP proteins play compensatory roles in morphogenesis and neuronal cell migration. *Genetics* **167**, 1165-1176.
Yu, S., Avery, L., Baude, E. and Garbers, D. L. (1997). Guanylyl cyclase expression in specific sensory neurons: a new family of chemosensory receptors. *Proc. Natl. Acad. Sci. USA* **94**, 3384-3387.